

PAPER • OPEN ACCESS

## Physical properties of calcium fluoride nanopowder produced by the method of evaporation by pulsed electron beam in a low-pressure gas

To cite this article: S Yu Sokovnin *et al* 2019 *J. Phys.: Conf. Ser.* **1281** 012079

View the [article online](#) for updates and enhancements.



**IOP | ebooks™**

Bringing together innovative digital publishing with leading authors from the global scientific community.

Start exploring the collection—download the first chapter of every title for free.

# Physical properties of calcium fluoride nanopowder produced by the method of evaporation by pulsed electron beam in a low-pressure gas

S Yu Sokovnin<sup>1,2</sup>, V G Il'ves<sup>2</sup> and M A Uimin<sup>1,3</sup>

<sup>1</sup> Ural Federal University, Yekaterinburg, Russia

<sup>2</sup> Institute of Electrophysics UB RAS, Yekaterinburg, Russia

<sup>3</sup> Miheev Institute of Metal Physics Ural Branch RAS, Yekaterinburg, Russia

E-mail: sokovnin@iep.uran.ru

**Abstract.** Mesoporous CaF<sub>2</sub> nanopowders with the specific surface area up to 88.7 m<sup>2</sup>/g have been produced by the evaporation by a pulsed electron beam in vacuum. The influence of thermal annealing in air on the size and morphology of CaF<sub>2</sub> nanoparticles and their magnetic, luminescence, and texture characteristics has been studied. Ferromagnetism of CaF<sub>2</sub> nanopowders was discovered for the first time. The influence of radiation defects (CaF<sub>2</sub> dye centers) on magnetic properties of CaF<sub>2</sub> nanoparticles has been examined.

## 1. Introduction

Nanofluorides of alkali-earth metals are promising for applications as catalysts and photonic materials, in particular, precursors of optical ceramics, as well as materials for biomedical applications. Different methods of production of CaF<sub>2</sub> nanoparticles, first of all, chemical ones are known [1]. Physical methods of obtaining fluoride nanopowders are poorly developed because they are hard to implement [2].

The objective of this paper was to produce the CaF<sub>2</sub> nanopowders by the method of evaporation by a pulsed electron beam in vacuum [3] and to study the structure, morphology, magnetic, luminescent, and texture properties of produced nanopowders.

## 2. Experimental

Targets of highly pure CaF<sub>2</sub> powders (TU 6-09-2412-84) were made at a hand press. Compacts were sintered in air at a temperature of 900 °C. The regime of target evaporation at the Nanobim-2 setup and nanopowder collection, as well as methods of nanopowder diagnostics, is described in [4]. CaF<sub>2</sub> nanopowders were annealed in alundum crucibles at a temperature of 200, 400, and 900 °C for 10 min. From here on, nanopowder specimens before and after annealing are designated as S0, S200, S400, and S900, respectively.

## 3. Results and discussion

The X-ray phase analysis has shown that all the nanopowders are single-phase; only fluorite is present. The lattice parameters of initial and annealed nanopowders are given in table 1. The texture analysis (table 1) has shown that the adsorption/desorption isotherms of S0 and S200 specimens correspond to the IV type of isotherms according to the IUPAC classification, which is indicative of the mesoporous



type of nanopowders. A significant increase in the specific surface of  $\text{CaF}_2$  nanopowders after annealing at a temperature of 200 °C was discovered (table 1). It should be noted that earlier we have observed the similar increase in the specific surface in the  $\text{BaF}_2$  nanopowder after annealing [4]. The annealing at 900°C has led to an increase in the particle size, which is confirmed by the data of X-ray phase analysis (decrease in FWHM of diffraction peaks) and to the loss in mesoporosity of the S900 specimen.

**Table 1.** Crystallographic and texture properties of  $\text{CaF}_2$  NPs.

Sample	$a$ , nm	FWHM	$S_{\text{BET}}$ , ( $\text{m}^2/\text{g}$ )	$V_{\text{p-total}}$ ( $\text{cm}^3/\text{g}$ )	$D_{\text{BJH}}$ (nm)
target	-	-	18.5	0.127	24.9
S0	5.4606 (6)*	0.141 (1)	64.3	0.25	21
S200	5.4582 (5)	0.22 (3)	88.7	0.66	29
S900	5.4588 (6)	0.101 (4)	1.11	0.0025	37

\*– measurement error in parentheses, FWHM – full width at half maximum;  $V_{\text{p-Total}}$  – total pore volume,  $D_{\text{BJH}}$  – average pore diameter,  $S_{\text{BET}}$  – specific surface.

The data of energy dispersion X-ray analysis (EDX) analysis (table 2) are indicative of the absence of any magnetic admixtures (Fe, Co, and Ni) in the specimens. Foreign carbon and oxygen could be adsorbed from the vacuum oil vapor in the evaporation chamber and the environment atmosphere in the process of specimen collection and storage. To be noted is the pronounced stoichiometric impurity in the specimens. The both specimens include excess calcium. The data of element mapping of light elements (F, O, C) have shown their uniform distribution over the analyzed parts of the S0 and S200 specimens.

**Table 2.** Results of EDX analysis.

Element	Line type	wt. %		at. %	
		S0	S200	S0	S200
C	K series	2.55	3.24	6.01	7.35
O	K series	1.05	1.55	1.85	2.65
F	K series	30.57	33.46	45.59	48.01
Ca	K series	65.84	61.75	46.54	42.00
Total:		100.00	100.00	100.00	100.00

Upon the resolution of pulsed cathodoluminescence (PCL) spectra of nanopowders into Gaussians, we can see three bands (table 3) responsible for two types of F-centers with peaks lying nearby ~500 (third type), ~530 (fourth type), ~630 (fifth type). These bands are results of recombination processes.

The PCL spectra of the specimens annealed at 200 and 400 °C included a wide (FWHM ~230 nm) band nearby ~630 nm (table 3), which is shifted by 110–130 nm with respect to the target PCL spectrum including two neighbor peaks. The third and fourth peaks of the PCL spectra of the target nanopowder specimens annealed at a temperature of 200 and 400 °C remain practically unchanged at annealing with allowance made for the approximation errors, whereas the fifth peak changes considerably in amplitude (with respect to the fourth peak, table 3) keeping the large width. After annealing at 900 °C, the third peak decreases drastically, while the fourth and fifth peaks practically disappear, merging into a single wide band nearby ~650 nm, and a new band appears nearby ~713 nm.

In our opinion, F-centers, whose number increases at annealing, are responsible for the bands at ~530 and ~630 nm. These bands can be caused by delocalization of hole centers and their recombination with F-centers [5].

The initial nanopowder (S0) has demonstrated the ferromagnetic (FM) behavior (figure 1). The literature data on this effect are lacking. The appearance of the FM response can be explained by

formation of structure and radiation defects (F-centers and others) just in the bands nearby ~530 and ~630 nm.

**Table 3.** Results of PCL analysis of the specimens.

Specimen	A3, a.u.	$\lambda$ 3, nm	FWHM3, nm	A4, a.u.	$\lambda$ 4, nm	FWHM4, nm	A5, a.u.	$\lambda$ 5, nm	FWHM5, nm	A5/A 4
target	1331	502	48	1992	522	92	-	-	-	
S0	702	498	50	602	532	114	240	637	229	0,4
S200	1242	497	64	799	544	101	586	627	275	0,73
S400	1426	499	65	1360	524	164	503	678	230	0,37
S900	236	486	154	727	673	120	872	713	138	1,2

Here, A are amplitudes,  $\lambda$  are peak wavelengths and FWHM is full width at half maximum of Gaussians.

A feature of the generated nanopowders is the presence of a large number of structure defects of various types [3] and radiation defects (~30 Gy) induced by the bremsstrahlung radiation of the evaporating electron beam. Therefore, by analogy with the model [6], we can assume that just fluoride vacancies take part in some way in formation of the ferromagnetic response in the S0 and S200 specimens.

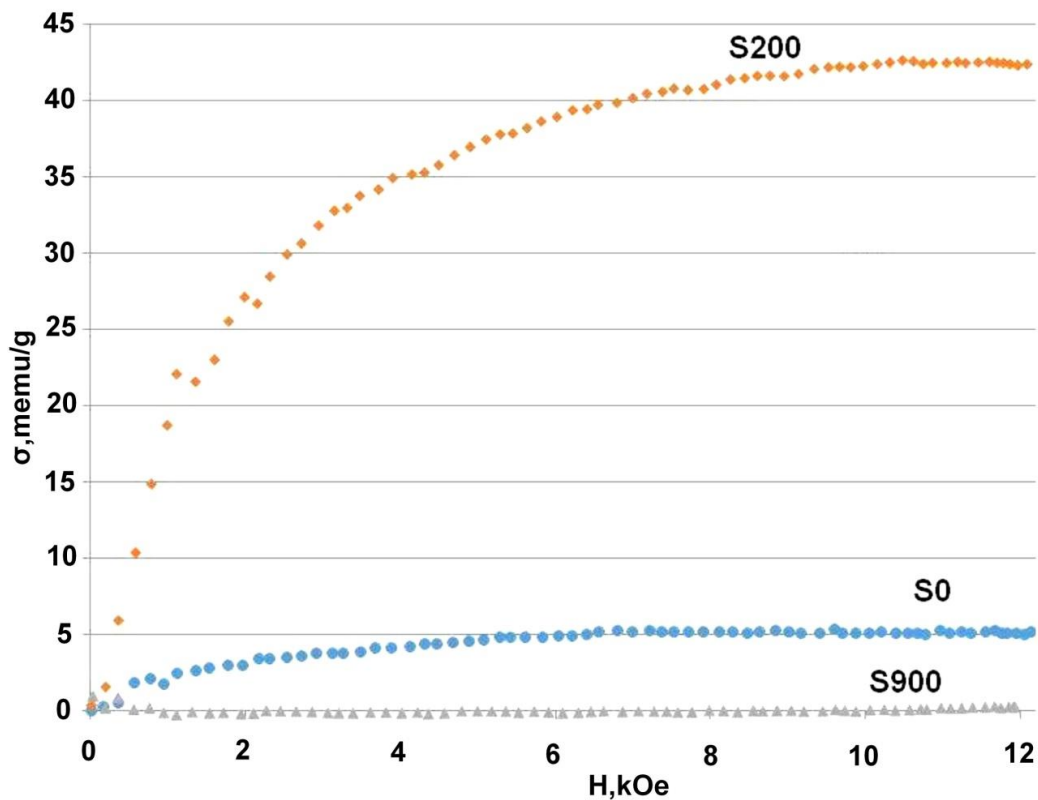


**Figure 1.** Magnetization curves of  $\text{CaF}_2$  specimens before and after annealing.

#### 4. Conclusions

The analysis of the PCL spectra and magnetization curves of the  $\text{CaF}_2$  specimens suggests the presence of correlation between them. The S0 specimen demonstrates the FM response, which increases after annealing in air at a temperature of 200 °C. At the same time, the PCL intensity at the bands nearby ~530 and ~630 nm increases drastically, while their mutual intensity changes. This fact

confirms that just these bands are responsible for the defect nature of magnetization. A drastic increase in the FM response and the emission intensity of the S200 specimen can be attributed to the removal of water adsorbed in mesopores of the S0 specimen. The annealing at 900 °C resulted in the vanishing of not only the FM response in the S900 specimen, but also the bands at ~530 and ~630 nm responsible for the surface dye centers. The vanishing of the FM response and appearance of the new band in the PCL spectrum (713) in the S900 specimen can be explained by the phase transformation of the initial single-phase specimen into the two-phase  $\text{CaF}_2$ -CaO specimen as a result of oxidation of metal Ca nanoparticles present in the S0 specimen.

The annealing of the S400 specimen resulted in some decrease of the FM response, whereas the cathodoluminescence intensity did not decrease. However, dye centers in the S400 specimen practically disappear (the plum color of the S0 specimen transforms into the white color), which is indicative of the complex mechanism of formation of FM response in  $\text{CaF}_2$ , only partially depending on the presence of radiation dye centers.

It is possible that the intensification of the FM response in the  $\text{CaF}_2$  nanopowder upon the annealing in the oxygen-containing environment follows the mechanism similar to that described in [7, 8] with participation of oxygen vacancies (in our case, fluoride vacancies). This fact calls for further investigations.

### Acknowledgment

This work was performed within the subject of the state task [0389-2015-0026]; was partial supported by the Russian Foundation for Basic Research [18-08-00514].

### References

- [1] Kuznetsov S, Yarotskaya I, Fedorov P, Voronov V, Lavrishchev S, Basiev T and Osiko V 2007 *Russ. J. Inorg. Chem.* **52** 315–20
- [2] Osipov V, Lisenkov V, Platonov V and Tikhonov E 2018 *Quant. Electron.* **48** 235–43
- [3] Sokovnin S and Ilves V 2012 *Ferroelectrics* **436** 101–7
- [4] Sokovnin S, Ilves V, Zuev M and Uimin M 2019 *Tech. Phys. Lett.* **44** 765–8
- [5] Antonyak O, Vistovskyy V, Zhyshkovych A and Kravchuk I 2015 *J. Lumin.* **67** 249–53
- [6] Singhal R, Kumari P, Samariya A, Kumar S, Sharma S, Xing Y and Saitovitch E 2010 *Appl. Phys. Lett.* **97** 172503
- [7] Gao D, Yang Z, Zhang J, Yang G, Zhu Z, Qi J, Si M and Xue D 2011 *AIP Advances*, **1** 042168
- [8] Ahmed S, Viboon P, Ding X, Bao N, Du Y, Herng T, Ding J and Yi J 2018 *J. Alloys Compd.* **746** 399–404